Vietnam Journal of Earth Sciences, 47(4), 542–564, https://doi.org/ 10.15625/2615-9783/23665

Vietnam Journal of Earth Sciences
https://vjs.ac.vn/index.php/jse

Spatiotemporal analysis of sea surface temperature and chlorophyll-a variability under ENSO-IOD influence in the Southern Madura Strait, Indonesia

Amir Yarkhasy Yuliardi[1*], Gandhi Napitupulu[2,3], Herlambang Aulia Rachman[4], Harmon Prayogi[5], Marita Ika Joesidawati[6], Viv Djanat Prasita[7]

[1]*Faculty of Fisheries and Marine Science, Universitas Jenderal Soedirman, Purwokerto, 53122, Indonesia*
[2]*Faculty of Earth Science and Technology, Bandung Institute of Technology, Cirebon, 45162, Indonesia*
[3]*Faculty of Earth Sciences and Technology, Bandung Institute of Technology, Bandung, 40132, Indonesia*
[4]*Faculty of Agriculture, University of Trunojoyo Madura, Bangkalan, 69162, Indonesia*
[5]*Faculty of Mathematics and Natural Sciences, Universitas Negeri Surabaya, Surabaya, 60231, Indonesia*
[6]*Faculty of Fisheries and Marine, Universitas PGRI Ronggolawe, Tuban, 62391, Indonesia*
[7]*Faculty of Engineering and Marine Science, Universitas Hang Tuah, Surabaya, 60111, Indonesia*

Received 20 May 2025; Received in revised form 23 September 2025; Accepted 23 October 2025

ABSTRACT

A dynamic interplay between local oceanographic processes and large-scale climate drivers shapes tropical coastal ecosystems. Yet, their coupled responses remain poorly quantified in many regions of the Indonesian Maritime Continent. This study examines the spatiotemporal variability of sea surface temperature (SST) and chlorophyll-a concentrations in the southern Madura Strait, utilizing 15 years (2010–2024) of monthly MODIS-Aqua observations, in conjunction with Niño 3.4 and Dipole Mode Index (DMI) time series to characterize ENSO and IOD phases. Monthly climatologies revealed a pronounced SST annual cycle, with peak warming during December-February (DJF) and March-May (MAM) (±31°C) and basin-wide cooling during June-August (JJA, ±28°C). Chlorophyll-a exhibited strong spatial heterogeneity, with the highest biomass (>10 mg/m^3) consistently observed in the western sector during DJF and MAM, likely reflecting monsoon-driven circulation and terrestrial nutrient inputs. Composite analyses revealed that La Niña and negative IOD phases increased productivity through surface cooling and nutrient enrichment. In contrast, El Niño and positive IOD phases resulted in compound warming events that suppressed chlorophyll-a. Lagged correlation analyses further revealed that chlorophyll-a responses typically lag climate anomalies by one to two months, underscoring the temporally asynchronous nature of climate-ecosystem interactions. These results provide new process-based insights into how ENSO-IOD interactions regulate tropical coastal productivity, highlighting the importance of incorporating climate drivers and temporal lags into forecasting and adaptive fisheries management frameworks to maintain ecosystem resilience under future climate variability.

Keywords: El Niño southern oscillation, Indian ocean dipole, Sea surface chlorophyll-a, Sea surface temperature, Southern Madura strait.

1. Introduction

The Southern Madura Strait is one of the critical coastal areas in Indonesia, both ecologically and economically (Hidayah et al., 2020). This region is part of the Java Sea and the strategic Madura Strait, which supports fishing activities, maritime shipping, and the maritime industry (Hidayah & Wiyanto, 2021;

*Corresponding author, Email: amiryarkhasy@gmail.com

Fauzan et al., 2023). Oceanographically, this area exhibits complex dynamics due to the influence of seasonal winds, the Indonesian Throughflow, and freshwater inputs from major rivers on Java Island (Atmadipoera et al., 2023; Yuliardi et al., 2024; Atmadipoera et al., 2024). In addition to local factors, global phenomena such as the El Niño-Southern Oscillation (ENSO) and the Indian Ocean Dipole (IOD) also play a role in influencing sea surface temperature (SST) and chlorophyll-a concentration dynamics, which are key indicators of primary productivity and water health (Toding et al., 2022; Simanjuntak et al., 2022; Ismunarti et al., 2023; Rachman et al., 2024; Hanansyah et al., 2024).

The Southern Madura Strait (approximately 6.8–7.65°S and 112.5–114.5°E) is a shallow semi-enclosed basin with an average depth of less than 50 m, connected to the Bali Sea in the east and the Java Sea in the west. Several rivers, including Bengawan Solo and Porong, discharge into this region, supplying freshwater and nutrient inputs that significantly affect coastal water quality and productivity (Maulana et al., 2015). Seasonal monsoon circulation further modulates oceanographic conditions: the west monsoon (December-February/DJF) brings heavy rainfall and riverine input, while the east monsoon (June-August/JJA) is marked by drier conditions, stronger southeasterly winds, and enhanced mixing (Napitupulu, 2025a). Although the Southern Madura Strait lies north of the well-documented Java upwelling system, it may be indirectly influenced by wind-driven circulation and nutrient enrichment during the east monsoon. These combined factors create a highly dynamic system where local and remote processes interact (Karima et al., 2025).

Research on oceanographic parameters such as sea surface temperature (SST) and chlorophyll-a has been widely conducted to understand marine environmental dynamics and primary productivity in various coastal areas of Indonesia (e.g., Ningsh et al., 2013; Wirasatriya et al., 2021; Napitupulu, 2024). In the Southern Madura strait, studies have predominantly focused on chlorophyll-a distribution. For example, Taufiqurrahman and Ismail (2020) highlighted the role of eddy formations in enhancing chlorophyll-a concentrations in the Madura Strait, while Trinugroho et al. (2019) identified thermal fronts as physical drivers of chlorophyll-a variability. Semedi and Safitri (2015) utilized MODIS satellite data to estimate chlorophyll-a concentrations. They reported seasonal phytoplankton fluctuations, while Jaelani et al. (2016) and Watanabe et al. (2018) demonstrated the utility of Landsat 8 OLI and Sentinel-2A imagery in mapping chlorophyll-a and suspended particulate matter distributions.

Additionally, studies on physical parameters, such as sea surface temperature (SST), have been conducted in the Madura region. Haryanto et al. (2021) presented the SST variability patterns in East Java's coastal areas using multi-temporal satellite data, showing that significant temperature changes are closely related to ENSO phenomena. Research by Zainab et al. (2020) further observed the changes in temperature and salinity in the Bangkalan waters of Madura, noting that the influence of seasonal currents and tidal activity plays a crucial role in SST fluctuations. Another study by Andriani et al. (2024) analyzed the SST change patterns in the Southern Madura Strait using oceanographic model data from Marine Copernicus from 2013–2020. However, these studies tend to focus on a single parameter and have not simultaneously examined the relationship between temperature changes and biological parameters such as chlorophyll-a. Agung et al. (2018) analyzed the relationship between SST and chlorophyll-a to identify potential fish catch locations in the central Java waters. Meanwhile, outside of Indonesia, integrative approaches between SST and chlorophyll have been more widely explored. Poddar et al. (2019) and Cui et al. (2020) successfully developed satellite-based chlorophyll-a estimation models that account for complex oceanographic factors, including

sea surface temperature, currents, and water optical classification.

Despite these advancements, several research gaps remain. First, there is a lack of simultaneous integration of physical (SST) and biological (chlorophyll-a) parameters over broad spatial and extended temporal scales in the Madura Waters. Second, the application of high-resolution satellite data and advanced spatiotemporal analysis to assess the impacts of global climate phenomena, particularly ENSO and IOD, on oceanographic variability is still limited. Third, few studies have directly linked SST and chlorophyll-a variability to implications for marine productivity and coastal fisheries management. To address these gaps, this study employs a multi-temporal remote sensing approach to analyze the spatiotemporal variability of SST and chlorophyll-a. It investigates their relationship with ENSO and IOD events. The findings are expected to enhance our understanding of ecosystem dynamics in the Southern Madura Strait and provide a scientific basis for adaptive management strategies in response to climate variability and change.

2. Data and Method

2.1. Study Area

This study was conducted in the southern part of the Madura Strait, located between the eastern part of Java Island and Madura Island (Fig. 1). The region is a semi-enclosed, shallow coastal zone characterized by complex oceanographic processes influenced by tidal currents, river discharges, and monsoonal wind forcing. It is also subject to large-scale climate variability associated with ENSO and the Indian Ocean Dipole (IOD) (Dewi et al., 2020). The study area spans from 6.8° to 7.65°S and 112.5° to 114.5°E, encompassing both nearshore and offshore waters. Bathymetry is generally shallow (<50 m), with riverine inputs contributing freshwater and nutrients that can affect coastal productivity. Three observation points were selected at a latitude of 7.35°S with longitudes of 113.0°E, 113.5°E, and 114.0°E to represent the western, central, and eastern transects of the study area.

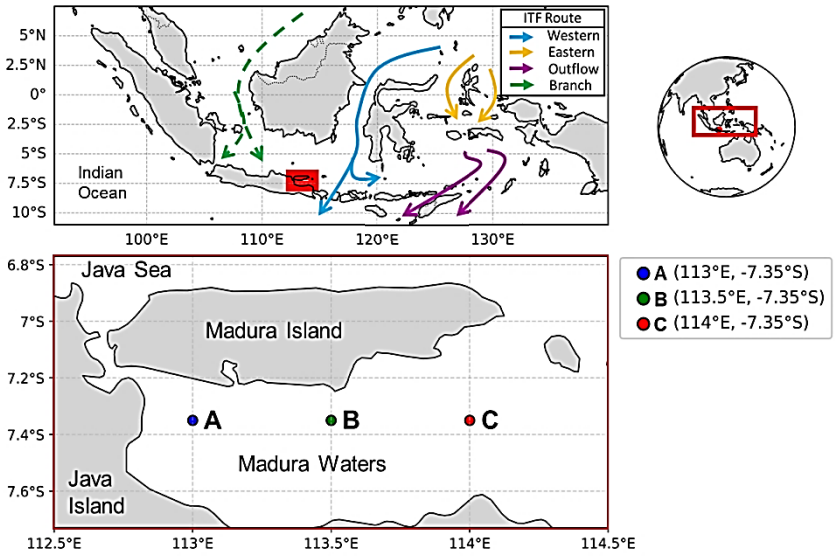

Figure 1. Study area of the Madura Strait Waters. Map of the Indonesian Seas with the red box highlighting the Madura Strait region. The inset on the right shows the location of the study area in a global context. Enlarged view of the Madura Strait showing three observation points: A (western, blue), B (central, green), and C (eastern, red), with their respective coordinates provided in the legend. Schematic of the Indonesian Throughflow (ITF) pathways is shown for context (modified from Xu et al., 2021)

2.2. Chlorophyll-a and Sea Surface Temperature dataset

Monthly composite data of SST and chlorophyll-a (Chl-a) were obtained from the Moderate Resolution Imaging Spectroradiometer (MODIS)-Aqua Level 3 product in NetCDF format. The dataset has a spatial resolution of 4 km and covers the period 2010–2024. The 4 km product was selected due to its relatively complete temporal coverage and reduce cloud obscuration by 5–14% compared to the 1 km product, which is often problematic in narrow coastal areas (Gao et al., 2010). While we acknowledge that the 4 km resolution may not fully resolve fine-scale nearshore features, previous studies have demonstrated the reliability of MODIS 4 km products for Indonesian coastal waters (e.g., Muskananfola & Wirasatriya, 2021; Akbar et al., 2024). This limitation is explicitly discussed in the manuscript, and we recommend future work to incorporate higher-resolution satellite data (e.g., MODIS 1 km, Sentinel-3 OLCI, VIIRS) and in situ validation (e.g., Harshada et al., 2021).

In addition, two global climate indices were used: (1) the Niño 3.4 Index (Oceanic Niño Index/ONI), representing central equatorial Pacific SST anomalies, obtained from the NOAA Climate Prediction Center (https://origin.cpc.ncep.noaa.gov/); and (2) the Dipole Mode Index (DMI), which characterizes the intensity of the Indian Ocean Dipole, obtained from the NOAA Physical Sciences Laboratory (https://psl.noaa.gov/).

2.3. Methods

This study employed a quantitative spatiotemporal approach to analyze chlorophyll-a and SST variability from 2010 to 2024. MODIS-Aqua Level 3 datasets in NetCDF (.nc) format were clipped according to the geographic boundaries of the study area. The data for chlorophyll-a and SST parameters consist of monthly composites with a spatial resolution of 4 km from the MODIS-Aqua sensor. To characterize the temporal variability, monthly climatological means and standard deviations were calculated from the 2010–2024 dataset, providing a detailed depiction of the average seasonal cycle and the magnitude of interannual variability for each calendar month.

Monthly climatological averages were computed by averaging each month across the 2010–2024 period, resulting in 12 monthly mean fields that represent the typical annual cycle of chlorophyll-a and SST. The interannual variability for each month was quantified using the corresponding standard deviation. This approach follows standard oceanographic climatology procedures and was adapted from Wirasatriya et al. (2017), with the monthly mean for each grid cell calculated as::

$$\bar{X}(x,y) = \frac{1}{n}\sum_{i=1}^{n} xi(x,y,t)$$

$$\underline{X}(x,y) = \frac{1}{n}\sum_{i=1}^{n} xi(x,y,t)$$

where the monthly climatological value at each coordinate point (x, y) is obtained by calculating the average of all parameter values at a specific time during the observation period. The number of data points used in this calculation (n) is adjusted according to the number of years within the study period. The time series of chlorophyll-a and SST are analyzed at three fixed coordinate points at latitude 7.35°S with variations in longitude at 113.0°E, 113.5°E, and 114.0°E. To fill in data gaps in the monthly time series, linear interpolation is applied using the nearest method. To gain a deeper understanding of the distribution of sea surface temperature (SST) and chlorophyll-a concentration at each observation point, a statistical distribution analysis is conducted using the Kernel Density Estimation (KDE) method. In the context of this study, KDE is used to evaluate

the distribution of SST and chlorophyll-a values over the monthly period (2010–2024) at the three observation locations, which are scattered longitudinally across the Southern Madura Strait. The estimation is performed using the Gaussian kernel function, which is mathematically formulated as follows (Gramacki, 2018):

$$\hat{f}_h(x) = \frac{1}{nh\sqrt{2\pi}} \sum_{i=1}^{n} exp\left(-\frac{1}{2}\left(\frac{x - x_i}{h}\right)^2\right)$$

where $\hat{f}_h(x)$ is the density estimate at point x, n is the total number of observation data, h is the bandwidth parameter that controls the smoothness of the estimation curve, and x_i represents each observation value in the dataset. In this study, the kernel function K used is the Gaussian kernel, which generally provides smooth estimation results and is suitable for continuous data such as sea surface temperature and chlorophyll-a. This KDE analysis is combined with histograms and boxplots to offer a comprehensive view of the distribution, central tendency, and the presence of extreme values (outliers) for each parameter.

Global climate indices (ONI and DMI) were plotted over the 2010–2024 period to identify the phases of ENSO and IOD. Phases corresponding to El Niño, La Niña, and positive or negative IOD events were highlighted to facilitate the evaluation of SST and chlorophyll-a variability in relation to global climate anomalies. Integrated visual analyses, combining spatial distribution maps and temporal plots, were conducted to elucidate the influence of seasonal and interannual variability on oceanographic conditions in the Madura Strait.

To assess the strength and timing of the relationship between climate indices and local oceanographic variability, lagged Pearson correlation analyses were performed between ONI/DMI and the SST and chlorophyll-a time series at the three observation points. Before conducting the correlation analysis, all time series were linearly detrended to remove long-term and seasonal trends. Correlations were calculated for lags ranging from 0 to +12 months to capture potential delayed responses.

$$r(\tau) = \frac{\sum_t (x(t) - \bar{x})\,(y(t+\tau) - \bar{y})}{\sqrt{\sum_t (x(t) - \bar{x})^2}\,\sqrt{\sum_t (y(t+\tau) - \bar{y})^2}}$$

To further investigate the influence of ENSO and IOD on oceanographic conditions, composite analyses were conducted to compare SST and chlorophyll-a anomalies during El Niño, La Niña, and neutral phases. Monthly anomalies were first categorized based on Oceanic Niño Index (ONI) and Dipole Mode Index (DMI) phases, and then averaged for each of the four climatological seasons: December-February (DJF), March-May (MAM), June-August (JJA), and September-November (SON). The resulting composites provide a spatial representation of temperature and chlorophyll-a differences between climate phases.

Composite differences were statistically tested using a two-tailed Student's *t*-test with a 95% confidence level to identify significant spatial patterns. This combined approach, seasonal composites, significance testing, and lagged correlations, provides a robust framework to isolate the impacts of ENSO and IOD on regional SST and chlorophyll-a variability and to infer the physical mechanisms

3. Results

3.1. Temporal Variability of Sea Surface Temperature and Chlorophyll-a

Figure 2 presents the temporal dynamics of global climate indices alongside key oceanographic parameters, namely, sea surface temperature (SST) and chlorophyll-a concentration in the Madura coastal waters from 2010 to 2024. Figure 2A illustrates the temporal fluctuations of the ENSO index (Niño 3.4, red line) and the Indian Ocean Dipole (IOD, shaded gray area). Figures 2B and 2C depict the variability of SST and

chlorophyll-a, respectively, at three fixed observation points along 7.35°S latitude, spanning longitudinally from 113°E to 114°E.

During the study period, a strong La Niña event was observed from late 2020 to early 2021, characterized by a significant decline in the Niño 3.4 index to approximately –1.8. This was followed by neutral conditions persisting from mid-2021 through early 2022. In early 2023, an El Niño episode intensified, peaking in the fourth quarter with a Niño 3.4 index exceeding +2.1. This El Niño event coincided with a positive IOD phase (approximately +1.0), forming an El Niño + positive IOD configuration typically associated with reduced precipitation and elevated SSTs across Indonesia, including East Java (Kurniadi et al., 2021).

Figure 2B illustrates the seasonal pattern of SST, with peak temperatures reaching approximately 31–32°C during the MAM and decreasing to around 28°C during the JJA. While the three observation points exhibit consistent trends over time, spatial variability remains evident: the western site (blue) generally displays higher SSTs compared to the eastern site (red). Notable temperature declines were observed in early 2021 and mid-2022, which correspond to La Niña phases and neutral-to-negative IOD conditions. In contrast, Fig. 2C highlights the more dynamic variability of chlorophyll-a concentrations. The highest values were recorded at the western station (113°E), exceeding 11 mg/m³ during several months in early 2023. The central (113.5°E) and eastern (114°E) locations exhibited lower and relatively stable chlorophyll-a levels, ranging from 0.2 to 1.5 mg/m³. The substantial increase in chlorophyll-a concentration at the western site is likely influenced by terrestrial nutrient inputs, carried by riverine runoff or surface flow (Rizqi et al., 2024). This process enriches the coastal waters of western Madura with nutrients, thereby supporting enhanced primary productivity in the region (Yuliardi et al., 2024).

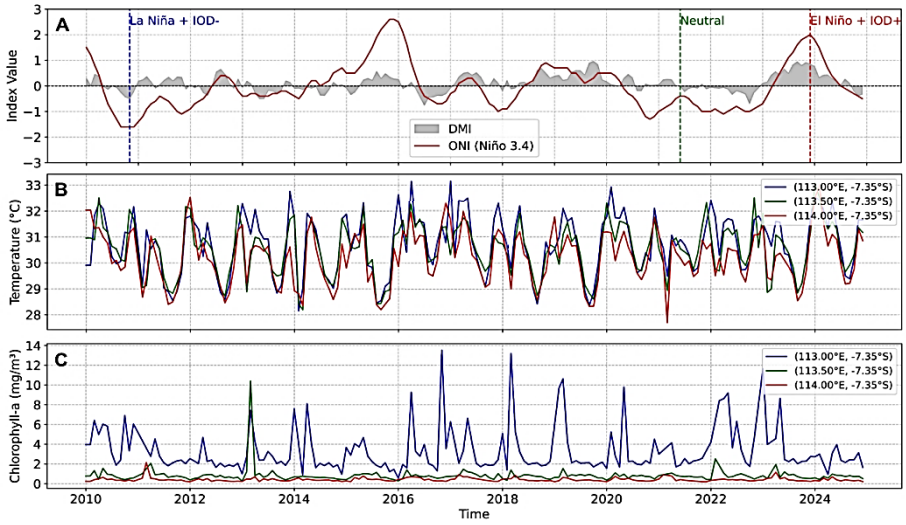

Figure 2. (A) IOD and ENSO indices from 2010 to 2024. Niño 3.4 index (red line) and Indian Ocean Dipole (IOD) index (DMI; shaded area) from 2010 to 2024, with markers for three key phases: La Niña + IOD-(November 2010), Neutral (June 2021), and El Niño + IOD+ (December 2023), (B)temporal variability of sea surface temperature (SST) and (C) chlorophyll-a concentration at three observation sites (western, central, and eastern) in the Madura coastal waters. Blue represents the western site, green the central, and red the eastern site

The temporal variability of SST and chlorophyll-a observed during the study period highlights the significant modulation of coastal oceanographic conditions by large-scale climate modes, such as ENSO and IOD. La Niña phases, characterized by cooler SSTs, appear to enhance nutrient availability, promoting phytoplankton growth, particularly in nearshore western Madura. Conversely, El Niño and positive IOD phases, associated with elevated SSTs, likely strengthen water column stratification, suppressing vertical nutrient fluxes and inhibiting primary productivity. The spatial disparity in SST and chlorophyll-a between western, central, and eastern sites highlights the combined influence of local terrestrial inputs and regional oceanographic gradients in shaping coastal ecosystem responses.

3.2 Statistical Distribution of Sea Surface Temperature and Chlorophyll-a

Figure 3 presents the frequency distribution (3A and 3B) and boxplot visualization (3C and 3D) of chlorophyll-a concentration and sea surface temperature (SST) at three observation points located along the fixed latitude of 7.35°S with longitudinal variations at 113°E, 113.5°E, and 114°E for the period 2010–2024. Figure 3A shows a histogram of chlorophyll-a distribution, highlighting pronounced spatial heterogeneity. The site at 113°E (blue) exhibits a markedly broad and positively skewed distribution, with the highest frequency occurring in the 1.5–2.5 mg/m³ range and values extending beyond ±10 mg/m³. The overlaid Kernel Density Estimation (KDE) curve further emphasizes the high variability observed at this location.

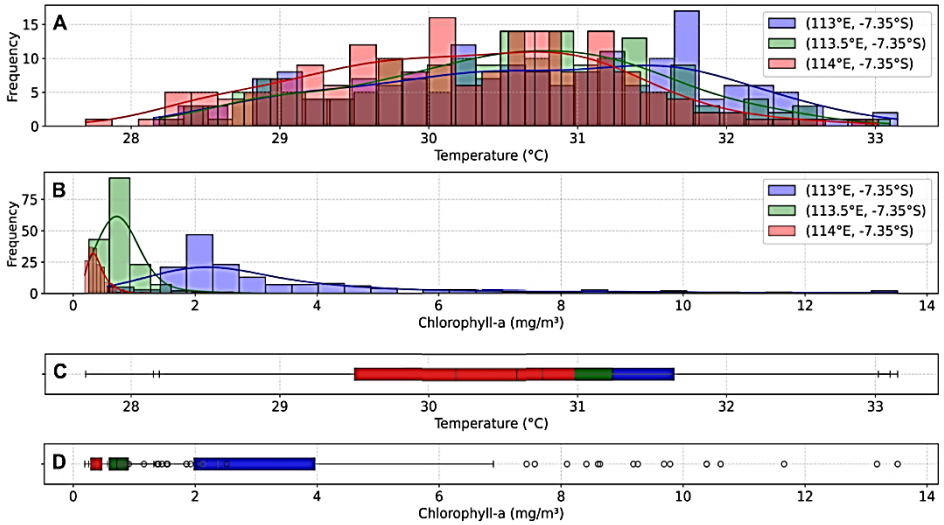

Figure 3. Frequency distribution and boxplots of chlorophyll-a (A, C) and sea surface temperature (B, D) at three locations along the -7.35° latitude between 2010 and 2024. Blue, green, and red represent the sites at 113°E, 113.5°E, and 114°E, respectively

Conversely, the sites at 113.5°E (green) and 114°E (red) exhibit narrower distributions, with chlorophyll-a concentrations predominantly below 1 mg/m³. The KDE curves indicate a leptokurtic distribution, suggesting stable oligotrophic conditions with minimal fluctuations in primary productivity. Figure 3B presents the SST histograms, which display more uniform patterns across all sites, yet still reveal systematic differences. Sea surface temperatures at all three locations ranged

between 28°C and 33°C during El Niño, with dominant frequencies concentrated in the 30–31°C range. The easternmost site, at 114°E (red), recorded the highest peak frequency within the 30.5–31.5°C interval, indicating a thermally stable and warmer water mass. The KDE curve for this location also displays a near-normal distribution skewed slightly to the right, while the distributions for the other two sites are marginally broader with a mode centered around 30–31°C.

The boxplot in Fig. 3C (chlorophyll-a) reinforces the patterns observed in the histograms, where the site at 113°E exhibits a wide interquartile range (IQR) and a median value of approximately 2 mg/m³, with several outliers exceeding 10 mg/m³, indicating extreme productivity events. In contrast, the central and eastern locations show much lower median values (<1 mg/m³) and narrower IQRs, confirming low-productivity conditions with minimal temporal variability. Figure 3D (SST boxplot) shows relatively uniform median temperatures across all sites; however, the 114°E location has the highest median SST and displays a more symmetrical and concentrated distribution. Several extreme temperature outliers are observed in the western and central sites, suggesting more dynamic thermal variability, likely driven by seasonal influences or surface current fluctuations (Napitupulu et al, 2025c). Overall, Fig. 3 highlights a consistent west-to-east spatial gradient in both chlorophyll-a and SST, reflecting distinct environmental conditions between the nearshore zone (113°E) and the more offshore eastern waters (114°E).

Overall, the statistical distribution patterns highlight a distinct west-to-east gradient in both chlorophyll-a and SST across the study area. The broad and positively skewed distribution of chlorophyll-a at the western site indicates a dynamic environment influenced by episodic nutrient inputs, likely from riverine runoff or coastal upwelling (Radjawane et al., 2024). In contrast, the central and eastern sites exhibit more stable oligotrophic conditions. Meanwhile, SST distributions suggest a slight eastward warming trend, reflecting a transition from dynamic nearshore environments to more thermally stable offshore waters (Napitupulu, 2025b). These findings underscore the importance of considering both spatial and temporal variability when assessing the vulnerability of coastal ecosystems to climatic and oceanographic perturbations.

3.3. Spatial Variability of Sea Surface Temperature and Chlorophyll-a

Figures 4 and 5 illustrate the monthly spatial distribution of sea surface temperature (SST) and chlorophyll-a concentrations, respectively, across the Madura coastal waters for the period 2010–2024. In contrast to the earlier seasonal composite, these figures resolve intra-annual variability at a monthly scale, enabling a more detailed examination of the physical-biological coupling. In Fig. 4, SST exhibited a distinct annual cycle with strong spatial gradients. Peak warming occurred during March-April and again from October to December, when SSTs frequently exceeded 32°C, especially along the western and southwestern coastal waters. In contrast, a marked basin-wide cooling was observed during June-August, when SST dropped to nearly 28°C across the central and eastern sectors. The transition months (May and September) showed intermediate temperatures, reflecting the onset and relaxation of monsoonal forcing. Panel B reveals that the highest SST variability (STD > 1.5°C) was concentrated in the western nearshore zone during January-March and October-December, suggesting the influence of strong heat fluxes, coastal upwelling/relaxation events, and river discharge that create localized thermal contrasts.

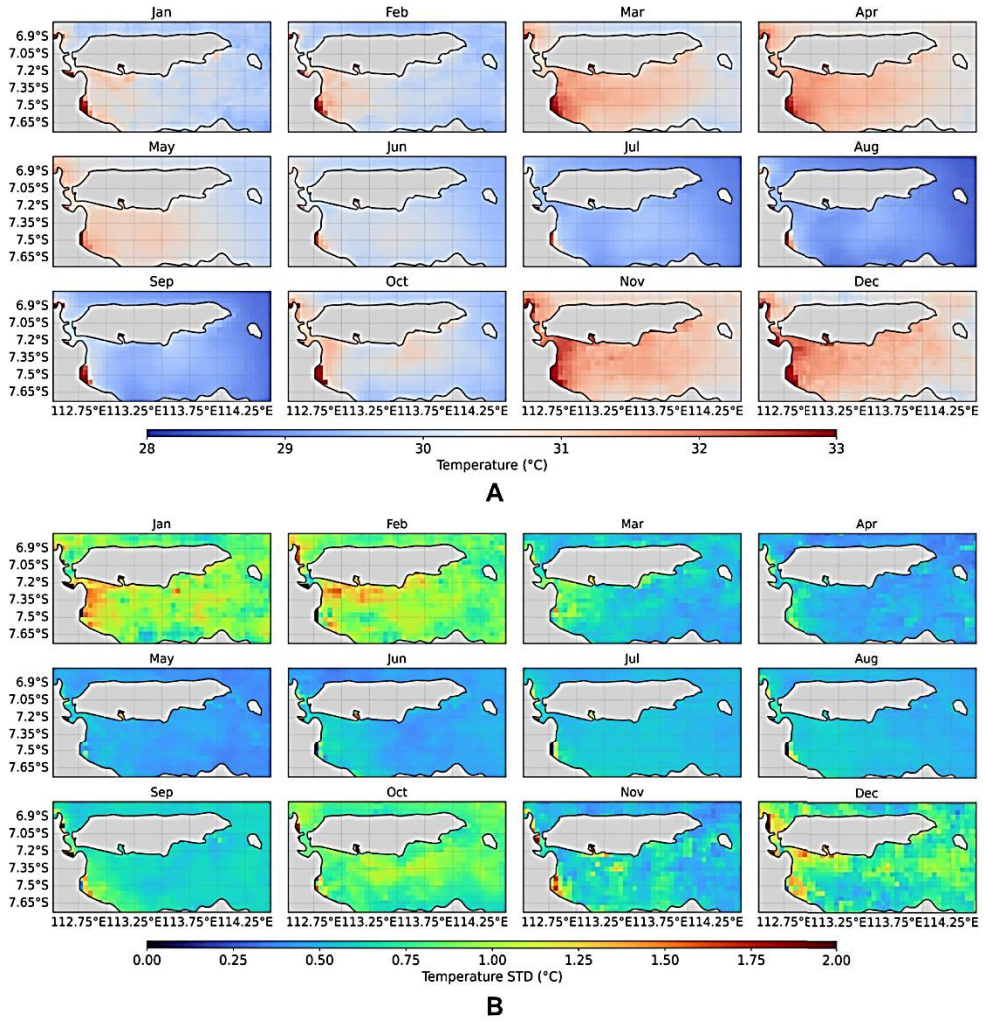

Figure 4. Monthly climatology of sea surface temperature (SST) in the Madura Strait for the period 2010–2024. (A) Mean monthly SST (B) Monthly standard deviation of SST

Figure 5 presents the monthly spatial patterns of chlorophyll-a concentration. Overall, phytoplankton biomass was lowest from January to March (< 2 mg/m³), coinciding with warm, stratified conditions. A rapid increase in chlorophyll-a began in April, with the most pronounced blooms occurring during June–September, when concentrations regularly exceeded 0–4 mg/m³ in the southern and southwestern nearshore waters. Elevated chlorophyll-a levels persisted from October to December, indicating that productivity remained high even after SST began to recover from its seasonal minimum. Panel B shows that variability was extreme in the southwestern coastal region (> 5 mg/m³), reflecting the episodic and spatially heterogeneous nature of nutrient inputs and biological responses.

The combined interpretation of Figs. 4 and 5 highlights a tight coupling between physical forcing and biological productivity in the Madura Strait. The southeast monsoon (JJA) drives significant surface cooling, likely through enhanced wind-driven mixing and upwelling, which increases the nutrient

supply and stimulates phytoplankton blooms. Conversely, during March-April and late in the year, warm SSTs and intensified stratification may limit vertical nutrient fluxes, leading to reduced chlorophyll-a levels. The concentration of both high SST variability and high chlorophyll-a variability along the western coast suggests that this area is susceptible to terrestrial runoff and nearshore circulation, which can modulate nutrient availability and promote localized productivity hotspots. This spatial heterogeneity has important implications for fisheries, as it may create persistent zones of high primary production that support higher trophic levels. These findings underscore the importance of monthly-resolved analyses for accurately capturing the timing and intensity of physical-biological interactions. Understanding these fine-scale seasonal dynamics is crucial for predicting ecosystem responses to future climate variability, including shifts in monsoon intensity and timing, and for developing adaptive coastal resource management strategies.

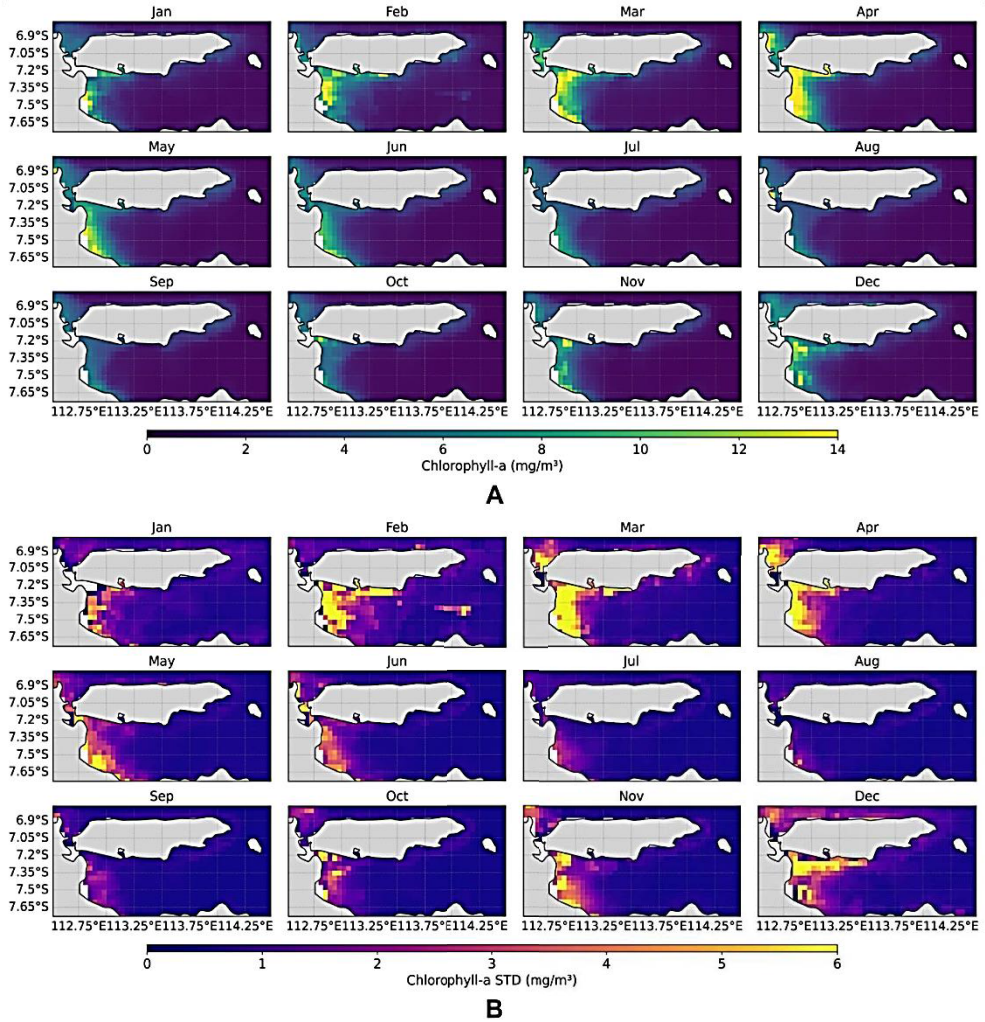

Figure 5. Monthly climatology of Chlorophyll-a in the Madura Strait for the period 2010–2024. (A) Mean monthly Chlorophyll-a (B) Monthly standard deviation of Chlorophyll-a

3.4. Relationship Between Chlorophyll-a, Sea Surface Temperature, and Global Climate Indices

Figure 6 illustrates the relationship between global climate anomalies (ENSO and IOD) and the variability of sea surface temperature (SST) and chlorophyll-a concentrations in the southern waters of Madura. In this updated analysis, three representative climate phases were selected from the extended 15-year record: La Niña combined with a negative IOD phase (November 2010), a Neutral condition (June 2021), and El Niño combined with a positive IOD phase (December 2023). Figures 6A–6C show the spatial distribution of SST, while Figs. 6D–6F present chlorophyll-a concentrations corresponding to each of these events. During the La Niña + IOD(-) phase (Figs. 6A and 6D), SST ranged from approximately 28.0°C to 30.0°C, with a pronounced cooling signal over the eastern sector of the study area. Concurrently, chlorophyll-a concentrations increased substantially along the western and southwestern coastal waters, frequently exceeding 9 mg/m³. This pattern indicates enhanced primary productivity, likely driven by wind-induced mixing and nutrient enrichment during the combined La Niña and negative IOD conditions. The spatial co-occurrence of cooler SST and elevated chlorophyll-a suggests a favorable environment for phytoplankton growth and potential upwelling-driven nutrient supply.

Under Neutral conditions (Figs. 6B and 6E), SST appeared relatively homogeneous, ranging between 29.0°C and 31.0°C across the entire basin. Chlorophyll-a concentrations were generally low (< 3 mg/m³), with limited patches of slightly elevated values along the southern coastal strip. These conditions reflect a more stratified water column and reduced nutrient availability. In contrast, during the El Niño + positive IOD phase (Figs. 6C and 6F), SST exceeded 32.0°C across most of the study area, with the warmest anomalies concentrated in the central and eastern sectors. Chlorophyll-a concentrations showed a marked decline, dropping below 1 mg/m³ over large portions of the basin, with only small pockets of elevated values persisting near the western coastline. This strong negative response of phytoplankton biomass supports the interpretation that extreme warming during El Niño + IOD(+) events enhances thermal stratification, suppresses vertical mixing, and limits nutrient flux into the euphotic zone (Zhang et al., 2014; Liu et al., 2024).

Figures 6G–6H summarize the spatially aggregated SST and chlorophyll-a responses during the three phases using boxplots. The distributions clearly show that La Niña + IOD(-) events are associated with the lowest SST and highest chlorophyll-a levels, while El Niño + IOD(+) events exhibit the highest SST and the lowest chlorophyll-a concentrations. Neutral conditions fall between these two extremes, confirming the modulation of local physical-biological interactions by large-scale climate variability. Overall, the contrasting impacts of La Niña and El Niño + IOD(+) highlight the significant sensitivity of the Madura coastal system to climate modes. Cooler SSTs during La Niña foster enhanced productivity, particularly near terrestrial nutrient sources along the western coast, whereas extreme warming during El Niño and positive IOD phases suppress nutrient availability and phytoplankton growth. These findings are consistent with broader Indo-Pacific patterns and highlight the importance of considering ENSO-IOD interactions when evaluating ecosystem responses and planning coastal resource management in a changing climate.

4. Discussions

The variability of chlorophyll-a concentrations in the study area is closely

linked to sea surface temperature (SST) dynamics and large-scale climate phenomena such as ENSO and the Indian Ocean Dipole (IOD) (Seprianto et al., 2016; Rachman et al., 2024). During the La Niña period (2010–2021), the decrease in SST corresponded with a marked increase in chlorophyll-a, particularly along the western coast. Conversely, during the strong El Niño event of 2023, which coincided with a positive IOD phase, SST rose above 31°C, followed by a sharp decline in chlorophyll-a levels. This pattern suggests that elevated temperatures may inhibit vertical mixing and restrict nutrient availability in the surface layer, thereby suppressing phytoplankton productivity (Hu et al., 2021; Fernández-González et al., 2022).

In addition to global-scale climate drivers, spatial variability in chlorophyll-a across different locations reflects the influence of local oceanographic processes. The western region (113°E) consistently recorded the highest concentrations and greatest fluctuations in chlorophyll-a, which may be attributed to the presence of coastal currents, seabed morphology, or nutrient inputs from terrestrial sources (Abreu et al., 2010; Neto et al., 2015; Semedi & Safitri, 2015). In contrast, the central and eastern regions displayed relatively low and stable chlorophyll-a concentrations throughout the year, likely reflecting the dominance of more stable regional physical processes. Overall, these findings underscore the significant impact of global climate variability, while also highlighting the importance of local oceanographic conditions in shaping primary productivity in the Madura coastal waters.

The spatial variability of chlorophyll-a and SST reveals a consistent longitudinal gradient, with the western region (113°E) generally exhibiting higher primary productivity compared to the eastern area. This pattern may be attributed to local oceanographic dynamics, such as coastal currents, terrestrial nutrient transport, and the possible presence of localized upwelling mechanisms in the southwest of Madura (Wirasatriya et al., 2021). The higher variability observed in the western location also reflects a more dynamic environment, influenced by physical factors such as waves and currents, as well as external drivers like land-based runoff. In contrast, the warmer SSTs observed in the eastern region are indicative of a more thermally stable open-ocean condition, typically associated with oligotrophic environments (Duarte et al., 2013). This also corresponds to the lower chlorophyll-a concentrations recorded in this area. Such spatial patterns highlight potential differences in phytoplankton community structures and broader ecosystem conditions along the Madura coastline, underscoring the importance of incorporating spatial heterogeneity into coastal fisheries management and conservation strategies for marine ecosystems.

The chlorophyll-a distribution shown in Fig. 5 exhibits clear seasonal variability closely linked to physical oceanographic dynamics, such as surface currents and terrestrial nutrient input (Mandal et al., 2022; Sudradjat et al., 2024). During the JJA season, chlorophyll-a concentrations in the southern waters of Madura consistently increase, indicating substantial nutrient input from the land (Hidayah et al., 2016; Muhsoni et al., 2009). These nutrients are transported by the prevailing east monsoon currents toward the coastal zone, creating favorable conditions for the growth of phytoplankton. This finding aligns with Darmawan et al. (2021), who highlighted the role of riverine nutrient input and surface current dynamics in shaping elevated chlorophyll-a concentrations in the region. Furthermore, Taufiqurrahman and Ismail (2020) noted that the presence of eddy circulation induced by a deep basin in the

Madura Strait also contributes to the observed chlorophyll-a distribution patterns. This is particularly evident during the JJA season, when recirculating water masses dominate and enhance the spatial heterogeneity of chlorophyll-a in the region (Napitupulu, 2025b).

The results presented in Fig. 6 reinforce the significant influence of ENSO and IOD phenomena on sea surface temperature dynamics and marine productivity, as reflected by chlorophyll-a concentrations (Sambah et al., 2021; Simanjuntak & Lin, 2022). During La Niña events, nutrient availability increases, enhancing phytoplankton activity, as evidenced by elevated chlorophyll-a levels in coastal waters (Espinoza-Morriberón et al., 2025; Purba et al., 2025). In contrast, the El Niño + positive IOD phase results in warmer temperatures and reduced inflow of colder, nutrient-rich waters, leading to a substantial decline in primary productivity (Häder et al., 2014; Siswanto et al., 2020). The neutral phase reflects intermediate conditions in terms of both SST and chlorophyll-a concentrations. These findings confirm the tangible impact of global climate variability on coastal marine ecosystems (Sarma et al., 2015; Holbrook et al., 2020).

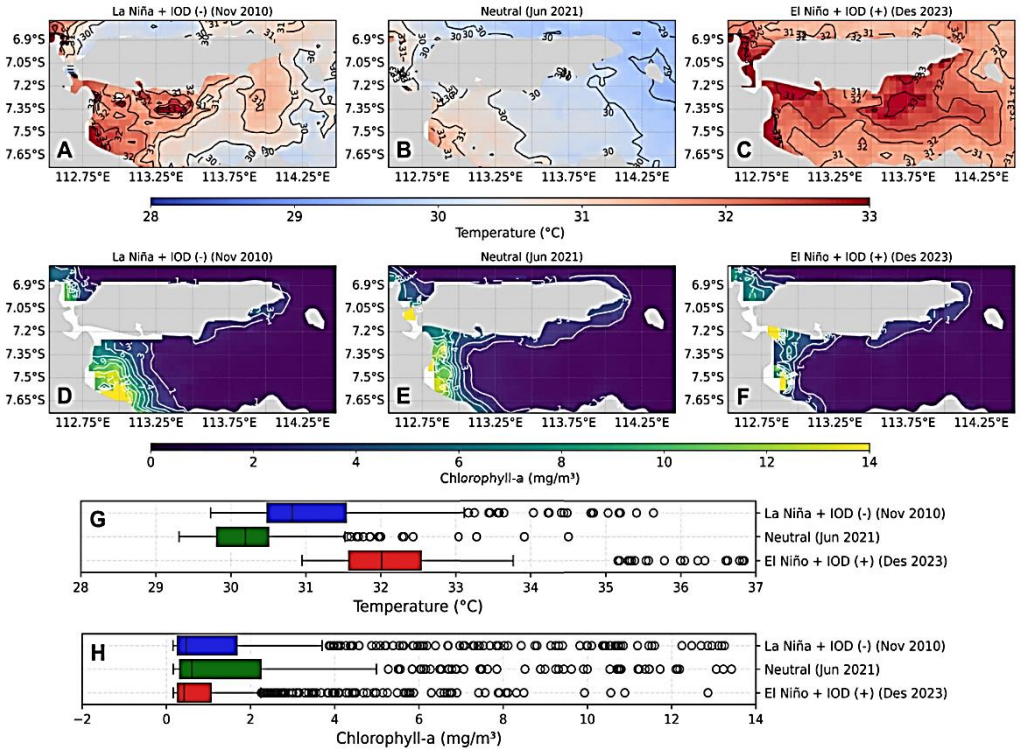

Figure 6. (A–C) Spatial distributions of sea surface temperature (SST), and (D-F) chlorophyll-a concentrations for each respective phase in the southern waters of Madura. Horizontal boxplot during the three phases, showing median, interquartile range, and variability across space of (G) SST and (H) chlorophyll-a

At a broader climatic scale, the study area lies within a tropical zone characterized by consistently warm temperatures (25–28°C) and high humidity throughout the year (Elko et al., 2022; Osland et al., 2022). According to the Köppen climate classification, tropical climates are categorized into three types: rainforest (Af), monsoon (Am), and savanna

(Aw) (Reddy, 2019; Kottek et al., 2006). Tropical rainforests, typically located near the equator, experience year-round rainfall, supporting dense, species-rich forests. Monsoon climates exhibit pronounced seasonal rainfall variation, favoring vegetation such as teak and bamboo (Liu & Zipser, 2005). In contrast, tropical savannas, characterized by distinct wet and dry seasons, are dominated by grasslands and drought-resistant species like acacia (Donato et al., 2011).

However, interannual climatic phenomena such as La Niña can significantly alter these stable tropical systems. During La Niña events, enhanced upwelling increases nutrient availability along tropical coastlines, boosting primary productivity and supporting the resilience of ecosystems such as coral reefs and mangroves (Khadami et al., 2025; Napitupulu et al., 2025). These productivity surges also provide significant socioeconomic benefits for coastal fisheries (Espinoza-Morriberón et al., 2025). Nonetheless, the sensitivity of tropical coastal ecosystems to both local and global environmental drivers underscores the need for adaptive management strategies that can accommodate both episodic variability and long-term climate change.

To further elucidate the temporal characteristics of the observed variability, Fig. 7 presents a lagged correlation analysis between ENSO and IOD indices with SST and chlorophyll-a at three representative locations. The study reveals that IOD exerts a more substantial and more immediate influence on SST than ENSO, with statistically significant negative correlations peaking at lags of −3 to 0 months. This indicates that basin-wide SST cooling generally precedes or coincides with negative IOD phases. Chlorophyll-a exhibits a delayed but inverse response to positive IOD events, with marked declines occurring up to two months after the peak, most prominently in the eastern and central sectors. These findings underscore that biological responses to climate anomalies, such as chlorophyll-a variability, often occur with temporal lags. This highlights the importance of integrated, high-resolution ocean observations to improve ecosystem-based forecasting and management of marine productivity (Schmidt et al., 2019).

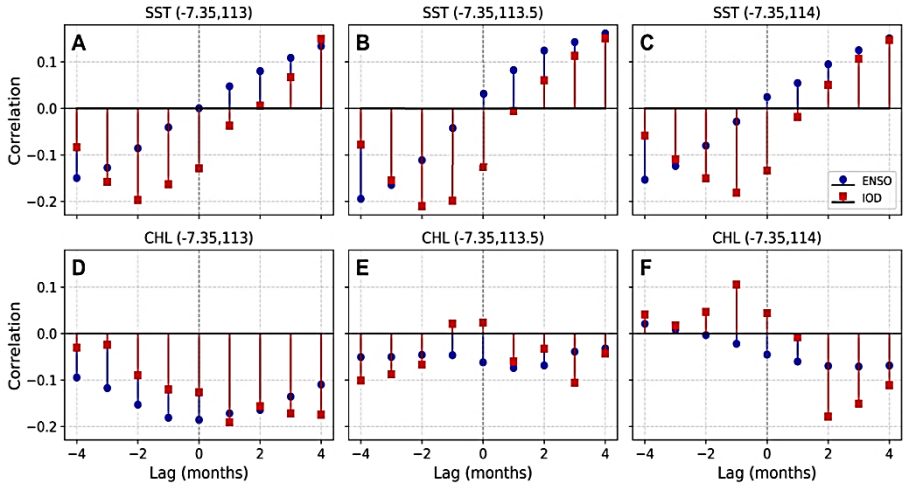

Figure 7. Lagged correlation between ENSO (blue circles) and IOD (red squares) indices with sea surface temperature (SST; panels A–C) and chlorophyll-a concentration (CHL; panels D–F) at three representative locations in the Madura coastal waters: (-7.35°S, 113°E), (-7.35°S, 113.5°E), and (-7.35°S, 114°E)

The seasonal composite analysis (Fig. 8) provides additional clarity on the differential impacts of ENSO phases on the regional hydrographic and biogeochemical environment. El Niño events consistently generated positive SST anomalies across all seasons, with the largest warming observed during DJF and MAM. In contrast, La Niña events induced significant basin-wide cooling, particularly during MAM and SON. The corresponding chlorophyll-a anomalies confirm that La Niña enhances primary productivity (especially during SON), consistent with intensified vertical mixing and nutrient replenishment during the southeast monsoon. In contrast, El Niño suppresses phytoplankton biomass, reflecting the effects of stronger stratification and nutrient limitation. These climate-ecosystem interactions underscore the importance of integrating observations and modeling to predict the seasonal responses of marine productivity under varying ENSO conditions (Capotondi et al., 2019).

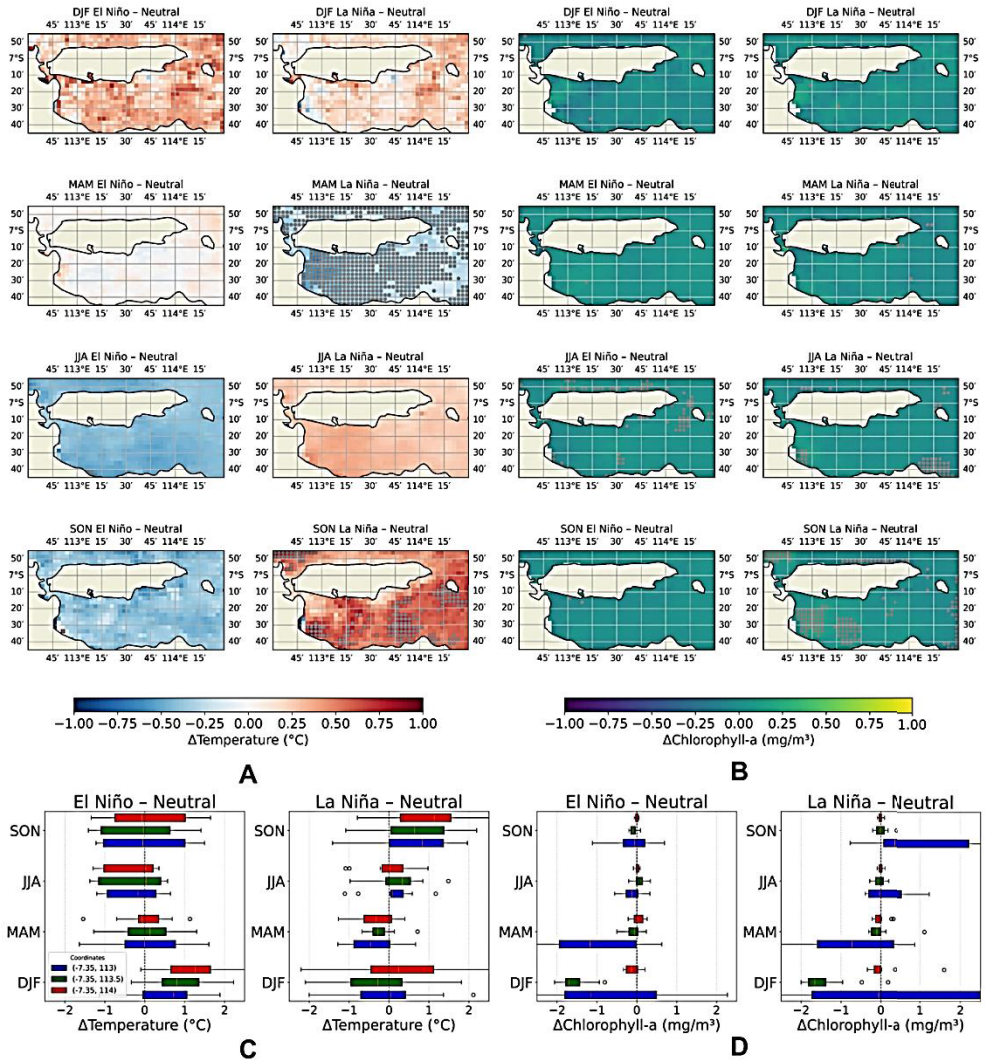

Figure 8. Seasonal composite anomalies of sea surface temperature (ΔSST; panels A, C) and chlorophyll-a (ΔCHL; panels B, D) relative to neutral conditions during El Niño (left columns) and La Niña (right columns) events over the 2010–2024 period

Figure 9 isolates the influence of the IOD and demonstrates that its impact is strongly seasonally modulated. Positive IOD events are associated with widespread surface warming and substantial reductions in chlorophyll-a concentrations, while negative IOD events produce significant cooling and enhance primary production, most notably during SON. These findings suggest that the IOD serves as a key modulator of SST and productivity, capable of either amplifying or attenuating the concurrent ENSO signal. For example, negative IOD phases can partially offset the warming associated with El Niño, whereas positive IOD phases reinforce warming during El Niño events, yielding compound extremes with disproportionately large ecological consequences. Positive and negative IOD events strongly modulate SST and marine productivity, amplifying or offsetting ENSO-related anomalies and producing compound ecological effects (Lehodey et al., 2020).

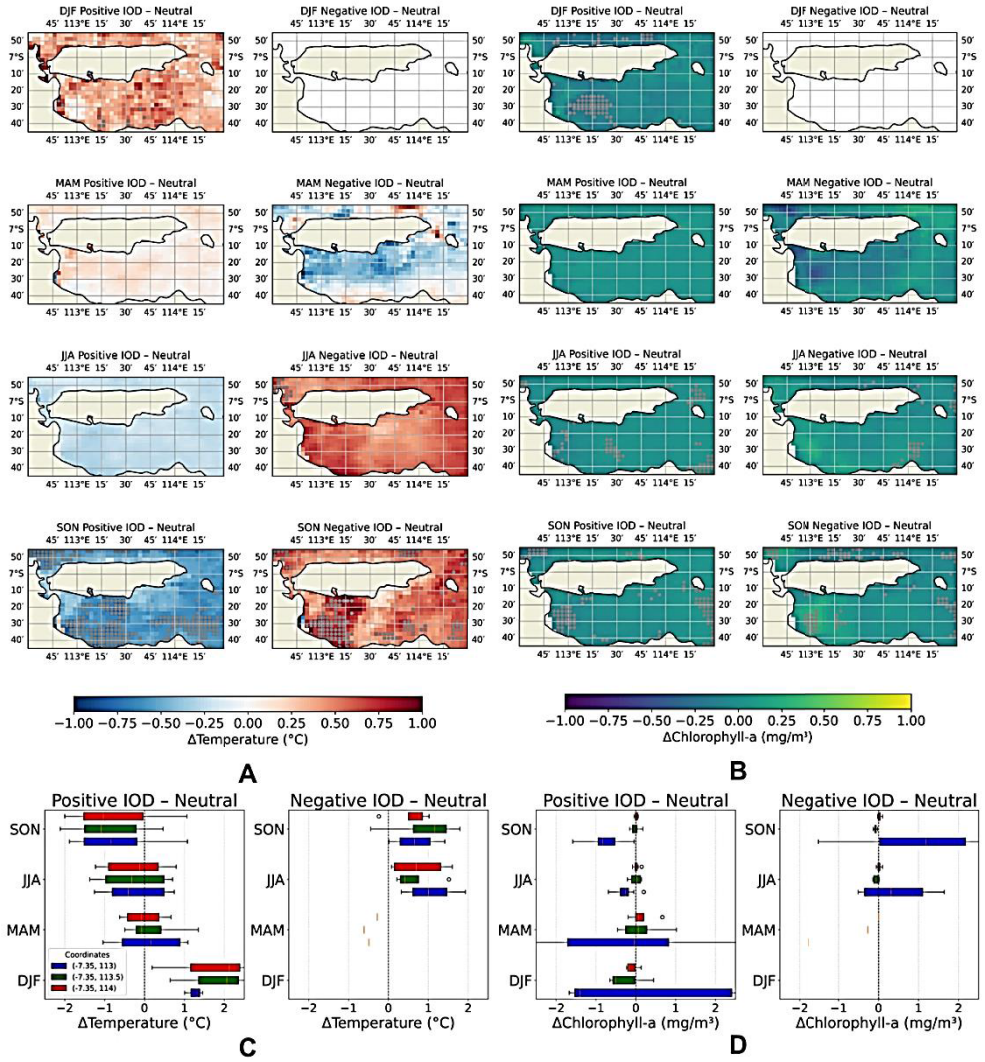

Figure 9. Seasonal composite anomalies of sea surface temperature (ΔSST; panels A, C) and chlorophyll-a (ΔCHL; panels B, D) relative to neutral conditions during positive (left columns) and negative (right columns) Indian Ocean Dipole (IOD) events for 2010–2024

Taken together, Figs. 7–9 collectively demonstrate that the variability of SST and chlorophyll-a in the Madura coastal waters is governed by a complex interplay between ENSO and IOD, modulated by their phase alignment, seasonal timing, and lagged effects. The most favorable conditions for phytoplankton blooms occur when La Niña coincides with negative IOD phases, resulting in extensive cooling, enhanced vertical mixing, and nutrient enrichment, whereas compound El Niño + positive IOD events produce exceptional warming that strongly suppresses primary productivity (Zhang et al., 2014; Liu et al., 2024). These interactions reveal the nonlinear nature of climate forcing on coastal ecosystems and emphasize the necessity of integrated seasonal forecasting frameworks that explicitly incorporate multiple climate modes when predicting ecosystem responses.

Despite the robustness of our multi-year satellite-based analysis, several limitations should be acknowledged. First, this study relies exclusively on MODIS-Aqua Level-3 products, which, while well-validated globally, may be subject to retrieval errors under persistent cloud cover and nearshore waters with complex optical properties. Second, the spatial resolution of the data (4 km) may not fully capture sub-mesoscale processes, such as localized upwelling cells, river plumes, and small-scale eddy activity, which can substantially influence nutrient dynamics and primary production in coastal settings. Third, the absence of concurrent in-situ measurements precludes direct validation of satellite-derived SST and chlorophyll a, which could help refine the interpretation of observed anomalies. Future work should combine long-term satellite observations with targeted field campaigns and high-resolution coupled physical-biogeochemical models to resolve fine-scale processes and assess their contributions to variability in primary productivity. Addressing these limitations will provide a more mechanistic and spatially explicit understanding of climate-ecosystem linkages, ultimately supporting more accurate prediction of coastal productivity under changing climate regimes.

Collectively, the results of this study provide a comprehensive understanding of the coupled physical-biological dynamics that have governed the Madura coastal system over the past 15 years. By combining climatological analysis, event-based composites, and lagged correlations, we demonstrate that both intra-annual and interannual variability are closely linked to the interplay between ENSO and IOD, with significant implications for ecosystem functioning and fisheries productivity. The clear correspondence between cooler ocean states and enhanced primary production highlights the potential vulnerability of this region to future climate change scenarios characterized by more frequent and intense marine heatwaves. These findings not only improve our mechanistic understanding of tropical coastal biogeochemistry but also provide actionable insights for fisheries management and coastal ecosystem conservation, underscoring the need for adaptive strategies that anticipate climate-driven changes in ocean productivity.

5. Conclusions

This study provides an integrated assessment of the spatial and temporal dynamics of sea surface temperature (SST) and chlorophyll-a concentrations in the southern waters of Madura Island, elucidating their links to both seasonal forcing and large-scale climate phenomena, including the El Niño-Southern Oscillation (ENSO) and the Indian Ocean Dipole (IOD). Our results reveal pronounced seasonal SST variability, with peak warming during DJF and MAM (>31°C) and minimum values during JJA and SON (~28°C), closely associated

with the regional monsoon system. Chlorophyll-a concentrations exhibited distinct seasonal and spatial heterogeneity, with the highest biomass consistently observed during DJF and MAM in the western sector (>10 mg/m^3), suggesting that terrestrial nutrient inputs and monsoon-driven circulation play a dominant role in enhancing primary productivity. Event-based and lagged analyses demonstrate that ENSO and IOD exert a strong, phase-dependent influence on regional oceanographic conditions. La Niña and negative IOD phases consistently induced basin-wide cooling and substantial increases in chlorophyll-a, whereas El Niño and positive IOD phases produced compound warming events that suppressed productivity. Lagged correlations further indicate that biological responses are delayed relative to climate anomalies, with chlorophyll-a changes often occurring one to two months after the peak of SST anomalies. These results highlight the nonlinear and temporally asynchronous nature of climate forcing on coastal ecosystems. Overall, this study underscores the dual control of local oceanographic processes and remote climate drivers on primary productivity in Madura's coastal waters. By integrating multi-temporal satellite observations with global climate indices, we provide new insights into how seasonality, phase alignment, and temporal lag of ENSO-IOD events collectively shape marine ecosystem dynamics. These findings have significant implications for climate-ready fisheries management, emphasizing the need for early-warning systems and adaptive strategies that account for compound climate extremes and their potential to modulate coastal productivity under future climate change scenarios.

Acknowledgements

The authors express their sincere appreciation to the NASA OceanColor Web for providing the MODIS-Aqua Level-3 Chlorophyll-a data, as well as to the National Weather Service NOAA and the NOAA Physical Sciences Laboratory (PSL) for access to the Niño 3.4 and Dipole Mode Index (DMI) datasets, which were instrumental in the global climate analysis conducted in this study. The authors also extend their gratitude to the reviewers for their constructive feedback, insightful comments, and valuable suggestions, which have significantly contributed to the refinement of the manuscript and the enhancement of the research findings presented.

References

Abreu P.C., Bergesch M., Proença L.A., Garcia C.A., Odebrecht C., 2010. Short-and long-term chlorophyll a variability in the shallow microtidal Patos Lagoon estuary, Southern Brazil. Estuaries and Coasts, 33, 554–569. Doi: 10.1007/s12237-009-9181-9.

Agung A., Zainuri M., Wirasatriya A., Maslukah L., Subardjo P., Suryosaputro A.A.D., Handoyo G., 2018. Analysis of the distribution of chlorophyll-a and sea surface temperature as potential fishing grounds (small pelagic fish) in Kendal waters, Central Java. Buletin Oseanografi Marina, 7(2), 67–74. Doi: 0.14710/buloma.v7i2.20378 (in Bahasa).

Akbar M.A., Sosaidi D.S., Napitupulu G., Tahir A.A.R., 2024. Response of upwelling parameter before, during, and after tropical cyclone (Case Study: Tropical Cyclone Marcus). Jurnal Meteorologi dan Geofisika, 25(1), 25–33. Doi: 10.31172/jmg.v25i1.1071.

Andriani R., Sari S.H.J., Yuniarti A., IkHarlyan L., Pranowo W.S., Fuad M.A.Z., Sartimbul A., 2024. Analysis of Water Temperature Variations in the Madura Strait Waters in 2013-2020 Using Data from Marine Copernicus. Techno-Fish, 114–125. Doi: 10.25139/tf.vi.8699 (in Bahasa).

Atmadipoera A.S., Natih N.M.N., Nugroho D., Zuraida R., Hartanto M.T., Syahdan M., 2024. Water mass exchange in triangle seas of the Java-Makassar-Flores (JMF): A modeling study. Continental Shelf Research, 275, 105225. Doi: 10.1016/j.csr.2024.105225.

Atmadipoera A.S., Nugroho D., Jaya I., Akhir M.F., 2023. Simulated seasonal oceanographic changes and their implication for the small pelagic fisheries in the Java Sea, Indonesia. Marine Environmental Research, 188, 106012. Doi: 10.1016/j.marenvres.2023.106012.

Capotondi A., et al., 2019. Observational needs supporting marine ecosystems modeling and forecasting: from the global ocean to regional and coastal systems. Frontiers in Marine Science, 6, 623. https://Doi.org/10.3389/fmars.2019.00623.

Cui T.W., Zhang J., Wang K., Wei J.W., Mu B., Ma Y., Zhu J.H., Liu R.J., and Chen X.Y., 2020. Remote Sensing of Chlorophyll a Concentration in Turbid Coastal Waters Based on a Global Optical Water Classification System. ISPRS Journal of Photogrammetry and Remote Sensing, 163, 187–201. Doi: 10.1016/j.isprsjprs.2020.02.017.

Darmawan A., Herawati E.Y., Azkiya M., Cahyani R.N., Aryani S.H., Hardiyanti C.A., Dwiyanti R.S.M., 2021. Seasonal monitoring of chlorophyll-a with landsat 8 oli in the madura strait, pasuruan, East Java, Indonesia. Geography, Environment, Sustainability, 14(2), 22–29. Doi: 10.24057/2071-9388-2020-199.

Donato D.C., Kauffman J.B., Murdiyarso D., Kurnianto S., Stidham M., Kanninen M., 2011. Mangroves among the most carbon-rich forests in the tropics. Nature Geoscience, 4(5), 293–297. Doi: 10.1038/ngeo1123.

Duarte C.M., Regaudie-de-Gioux A., Arrieta J.M., Delgado-Huertas A., Agustí S., 2013. The oligotrophic ocean is heterotrophic. Annual Review of Marine Science, 5(1), 551–569. Doi: 10.1146/annurev-marine-121211-172337.

Elko N., et al., 2022. Human and ecosystem health in coastal systems. Shore Beach, 90, 28. Doi: 10.34237/1009018.

Espinoza-Morriberón D., Mogollón R., Velasquez O., Yabar G., Villena M., Tam J., 2025. Dynamics of Surface Chlorophyll and the Asymmetric Response of the High Productive Zone in the Peruvian Sea: Effects of El Niño and La Niña. International Journal of Climatology, e8764. Doi: 0.1002/joc.8764.

Dewi Y.W., Wirasatriya A., Sugianto D.N., Helmi M., Marwoto J., Maslukah L., 2020. Effect of ENSO and IOD on the variability of sea surface temperature (SST) in java sea. In IOP Conference Series: Earth and Environmental Science. IOP Publishing, 530(1), 012007. Doi: 10.1088/1755-1315/530/1/012007.

Fauzan A., Sutanto R., Zaini A., 2023. Empowerment of Ujung-Kamal Sea Crossing Transportation as a Maritime Defense Strategy in the Madura Strait. Jurnal Kewarganegaraan, 7(1), 1186–1194. Doi: 10.31316/jk.v7i1.5258 (in Bahasa).

Fernández-González C., Tarran G.A., Schuback N., Woodward E.M.S., Arístegui J., Marañón E., 2022. Phytoplankton responses to changing temperature and nutrient availability are consistent across the tropical and subtropical Atlantic. Communications Biology, 5(1), 1035. Doi: 10.1038/s42003-022-03971-z.

Gao Y., Xie H., Yao T., Xue C., 2010. Integrated assessment on multi-temporal and multi-sensor combinations for reducing cloud obscuration of MODIS snow cover products of the Pacific Northwest USA. Remote Sensing of Environment, 114(8), 1662–1675. Doi: 10.1016/j.rse.2010.02.017.

Gramacki A., 2018. Kernel Density Estimation. In: Nonparametric Kernel Density Estimation and Its Computational Aspects. Studies in Big Data. Springer, Cham, 37. Doi: 10.1007/978-3-319-71688-6_3.

Häder D.P., Villafane V.E., Helbling E.W., 2014. Productivity of aquatic primary producers under global climate change. Photochemical & Photobiological Sciences, 13(10), 1370–1392. Doi: 10.1039/C3PP50418B.

Hanansyah M.P., Handoko E.Y., Muryono M., 2024. Spatio-temporal Variation of Chlorophyll-a around the Flores Sea, Java Sea, and Makassar Strait and its Relationship with Temperature and Salinity. In IOP Conference Series: Earth and Environmental Science. IOP Publishing, 1418(1), 012036. Doi: 10.1088/1755-1315/1418/1/012036.

Harshada D., Raman M., Jayappa K.S., 2021. Evaluation of the operational Chlorophyll-a product from global ocean colour sensors in the coastal waters, south-eastern Arabian Sea. The Egyptian Journal of Remote Sensing and Space Science, 24(3), 769–786. Doi: 10.1016/j.ejrs.2021.09.005.

Haryanto Y.D., Riama N.F., Agdialta R., Hartoko A., 2021. Sea Surface Temperature (SST) analysis during ElNiño-LaNiña in the Java Sea. In IOP Conference Series: Earth and Environmental Science. IOP Publishing, 716(1), 012006. Doi: 10.1088/1755-1315/716/1/012006.

Hidayah G., Wulandari S.Y., Zainuri M., 2016. Study of Horizontal Distribution of Chlorophyll-a in the Waters of the Silugonggo River Estuary, Batangan District, Pati. Buletin Oseanografi Marina, 5(1), 52–59. https://Doi.org/10.14710/buloma.v5i1.11296 (in Bahasa).

Hidayah Z., Wiyanto D.B., 2021. Geographic Information System Modeling for Mapping the Suitability of Madura Strait Waters and Coastal Areas. Rekayasa, 14(1), 17–25. Doi: 10.21107/rekayasa.v14i1.9987 (in Bahasa).

Hidayah Z., Nuzula N.I., Wiyanto D.B., 2020. Analysis of the sustainability of fisheries resource management in the Madura Strait waters of East Java. Jurnal Perikanan Universitas Gadjah Mada, 22(2), 101–111. Doi: 10.22146/jfs.53099 (in Bahasa).

Holbrook N.J., et al., 2020. ENSO-driven ocean extremes and their ecosystem impacts. El Niño southern oscillation in a changing climate, 409–428. Doi: 10.1002/9781119548164.ch18.

Hu Q., Chen X., He X., Bai Y., Gong F., Zhu Q., Pan D., 2021. Effect of El Niño-related warming on Phytoplankton's vertical distribution in the Arabian Sea. Journal of Geophysical Research: Oceans, 126(11), e2021JC017882. Doi: 10.1029/2021JC017882.

Ismunarti D.H., Rifa'i A., Munandar B., Wirasatriya A., Susanto R.D., 2023. Effect of Extreme ENSO and IOD on the Variability of Chlorophyll-a and Sea Surface Temperature in the North and South of Central Java Province. ILMU KELAUTAN: Indonesian Journal of Marine Sciences, 28(1). Doi: 10.14710/ik.ijms.28.1.1-11.

Jaelani L.M., Limehuwey R., Kurniadin N., Pamungkas A., Koenhardono E.S., Sulisetyono A., 2016. Estimation of TSS and Chl-a Concentration from Landsat 8-OLI: The Effect of Atmosphere and Retrieval Algoritm. IPTEK, The Journal for Technology and Science, 27(1), 16–23. Doi: 10.12962/j20882033.v27i1.1217.

Karima S., Ningsih N.S., Tisiana A.R., Napitupulu G., 2025. Water Mass Vertical Mixing in The Sulawesi Sea and Makassar Strait During the Second Transition Monsoon. Earth and Planetary Science, 4(1), 73–88. Doi: 10.36956/eps.v4i1.2061.

Khadami F., Suprijo T., Hidayat A.R., Radjawane I.M., Tarya A., Napitupulu G., 2025. Near-bed flow dynamics and bed shear stress in a mangrove-vegetated estuary. In IOP Conference Series: Earth and Environmental Science. IOP Publishing, 1464(1), 012014. Doi: 10.1088/1755-1315/1464/1/012014.

Kottek M., Grieser J., Beck C., Rudolf B., Rubel F., 2006. World map of the Köppen-Geiger climate classification updated. Doi: 10.1127/0941-2948/2006/0130.

Kurniadi A., Weller E., Min S.K., Seong M.G., 2021. Independent ENSO and IOD impacts on rainfall extremes over Indonesia. International Journal of Climatology, 41(6), 3640–3656. Doi: 10.1002/joc.7040.

Lehodey P., et al., 2020. ENSO impact on marine fisheries and ecosystems. El Niño Southern Oscillation in a changing climate, 429–451. https://doi.org/10.1002/9781119548164.ch19.

Liu C., Zipser E.J., 2005. Global distribution of convection penetrating the tropical tropopause. Journal of Geophysical Research: Atmospheres, 110(D23). Doi: 10.1029/2005JD006063.

Liu J., Deng J., Tang X., 2024. Reduction of thermal stratification due to global warming in winter and spring. Journal of Oceanology and Limnology, 1–15. Doi: 10.1007/s00343-024-4010-3.

Mandal S., Susanto R.D., Ramakrishnan B, 2022. On investigating the dynamical factors modulating surface chlorophyll-a variability along the south Java coast. Remote Sensing, 14(7), 1745. Doi: 10.3390/rs14071745.

Maulana M.A., Soemitro R.A.A., Mukunoki T., 2016. Assessment to the sediment concentration affected by river water current during dry and monsoon seasons at Kanor village-Bengawan Solo River. Japanese Geotechnical Society Special Publication, 2(72), 2484–2487. Doi: 10.3208/jgssp.INA-02.

Muhsoni F.F., Efendy M., Triajie H., 2009. Mapping of fishing ground locations and fisheries utilization status in the Madura Strait waters. Jurnal Fisika Flux: Jurnal Ilmiah Fisika FMIPA Universitas Lambung Mangkurat, 6(1), 50–64. Doi: 10.20527/flux.v6i1.3049 (in Bahasa).

Muskananfola M.R., Wirasatriya A., 2021. Spatio-temporal distribution of chlorophyll-a concentration, sea surface temperature and wind speed using aqua-modis satellite imagery over the Savu Sea, Indonesia. Remote Sensing Applications: Society and Environment, 22, 100483. Doi: 10.1016/j.rsase.2021.100483.

Napitupulu G., 2025a. Spatiotemporal variability of coastal upwelling in response to monsoonal forcing and semi-enclosed basins in the indonesian and adjacent seas. Ocean Dynamics, 75(7), 1–20. Doi: 10.1007/s10236-025-01706-2.

Napitupulu G., 2025b. Eddy-induced modulation of marine heatwaves and cold spells in a tropical region: a case study in the natuna sea area. Ocean Dynamics, 75(3), 28. Doi: 10.1007/s10236-025-01673-8.

Napitupulu G., 2025c. Influence of mesoscale eddies on marine cold spells and heatwaves in Arafura Sea. Marine Systems & Ocean Technology, 20(4), 44. Doi: 10.1007/s40868-025-00189-6.

Napitupulu G., 2024. Monthly variability of wind-induced upwelling and its impact on chlorophyll-a distribution in the Southern and Northern parts of the Indonesian Archipelago. Ocean Dynamics, 74(10), 859–878. Doi: 10.1007/s10236-024-01640-9.

Napitupulu G., et al., 2025. Impact of marine heatwaves and cold spells on coral reef ecosystem in a tropical region: a case study of Lombok Waters, Indonesia. Marine Systems & Ocean Technology, 20(1), 16. Doi: 10.1007/s40868-024-00160-x.

Neto J.L.R., Fragoso C.R., Malhado A.C., Ladle R.J., 2015. Spatio-temporal variability of chlorophyll-a in the coastal zone of northeastern Brazil. Estuaries and Coasts, 38, 72–83. Doi: 10.1007/s12237-014-9809-2.

Ningsih N.S., Rakhmaputeri N., Harto A.B., 2013. Upwelling variability along the southern coast of Bali and in Nusa Tenggara waters. Ocean Science Journal, 48, 49–57. Doi: 10.1007/s12601-013-0004-3.

Osland M.J., et al., 2022. The impacts of mangrove range expansion on wetland ecosystem services in the southeastern United States: Current understanding, knowledge gaps, and emerging research needs. Global Change Biology, 28(10), 3163–3187. Doi: 10.1111/gcb.16111.

Poddar S., Chacko N., Swain D., 2019. Estimation of Chlorophyll-a in Northern Coastal Bay of Bengal Using Landsat-8 OLI andentinel-2 MSI Sensors. Frontiers in Marine Science, 598(6), 1–11. Doi: 10.3389/fmars.2019.00598.

Purba N.P., Pranowo W.S., Ndah A.B., Nanlohy P., 2021. Seasonal variability of temperature, salinity, and surface currents at 0 latitude section of Indonesia seas. Regional Studies in Marine Science, 44, 101772. Doi: 10.1016/j.rsma.2021.101772.

Purba N., Akhir M., Faid G., Roseli N., Sinaga I., Faizal I., 2025. Stratified Ocean Chlorophyll-a and Nutrient Availability in the Eastern Tropical Indian Ocean during La Nina 2022-2023. Egyptian Journal of Aquatic Biology and Fisheries, 29(1), 297–320. Doi: 10.21608/ejabf.2025.404325.

Rachman H.A., Hidayah Z., Yuliardi A.Y., 2025. Dynamics of Sea Surface Temperature and Chlorophyll-a Concentration in Flores Sea Waters in Relation to ENSO and IOD Phenomena. Jurnal Kelautan Tropis, 28(1), 53–62. Doi: 10.14710/jkt.v28i1.25779 (in Bahasa).

Rachman H.A., et al., 2024. Dynamic of upwelling variability in southern Indonesia region revealed from satellite data: Role of ENSO and IOD. Journal of Sea Research, 202, 102543. Doi: 10.1016/j.seares.2024.102543.

Radjawane I.M., Saleh E., Napitupulu G., Abdillah M.R., Hassan M.A.M., 2024. Seasonal Variability of Sea Surface Chlorophyll-a at West Borneo Island. The Indonesian Journal of Geography, 56(1), 70–81. Doi: 10.22146/ijg.87713.

Reddy S., 2019. Four types of coastal habitats and why they matter. Mangroves, seagrass, salt marshes, and coral reefs sustain ocean life and help mitigate climate change. https://www.pewtrusts.org/en/research-and-analysis/articles/2019/05/31/four-types-of-coastal-habitats-and-why-they-matter.

Rizqi A.A., Ismunarti D.H., Maslukah L., 2024. Relationship of Chlorophyll-A to Environmental

Parameters in Morodemak, Central Java. Journal of Marine Research, 13(4), 713–720. Doi: 10.14710/jmr.v13i4.41159 (in Bahasa).

Sambah A.B., Wijaya A., Iranawati F., Hidayati N., 2021. Impact of ENSO and IOD on chlorophyll-a concentration and sea surface temperature in the Bali Strait. In IOP Conference Series: Earth and Environmental Science. IOP Publishing, 674(1), 012083. Doi: 10.1088/1755-1315/674/1/012083.

Sarma V.V.S.S., Paul Y.S., Vani D.G., Murty V.S.N., 2015. Impact of river discharge on the coastal water pH and pCO_2 levels during the Indian Ocean Dipole (IOD) years in the western Bay of Bengal. Continental Shelf Research, 107, 132–140. Doi: 10.1016/j.csr.2015.07.015.

Schmidt J.O., et al., 2019. Future ocean observations to connect climate, fisheries and marine ecosystems. Frontiers in Marine Science, 550(6). https://doi.org/10.3389/fmars.2019.00550.

Semedi B., Safitri N., 2015. Estimation of Chlorophyll-A Distribution in Madura Strait Waters Using Modis Satellite Imagery Data and In Situ Measurements During the East Season. Research Journal of Life Science, 2(1), 40–49. Doi: 10.21776/ub.rjls.2015.002.01.6 (in Bahasa).

Seprianto A., Kunarso K., Wirasatriya A., 2016. Study of the influence of El Niño Southern Oscillation (ENSO) and Indian Ocean Dipole (IOD) on the variability of sea surface temperature and chlorophyll-a in Karimunjawa waters. Journal of Oceanography, 5(4), 452–461. https://ejournal3.undip.ac.id/index.php/joce/article/view/16089 (in Bahasa).

Simanjuntak F., Lin T.H., 2022. Monsoon effects on chlorophyll-a, sea surface temperature, and ekman dynamics variability along the southern coast of lesser Sunda islands and its relation to ENSO and IOD based on satellite observations. Remote Sensing, 14(7), 1682. Doi: 0.3390/rs14071682.

Siswanto E., Horii T., Iskandar I., Gaol J.L., Setiawan R.Y., Susanto R.D., 2020. Impacts of climate changes on the phytoplankton biomass of the Indonesian Maritime Continent. Journal of Marine Systems, 212, 103451. Doi: 10.1016/j.jmarsys.2020.103451.

Somavilla R., González-Pola C., Fernández-Diaz J., 2017. The warmer the ocean surface, the shallower the mixed layer. H ow much of this is true?. Journal of Geophysical Research: Oceans, 122(9), 7698–7716. Doi: 10.1002/2017JC013125.

Sudradjat A., Muntalif B.S., Marasabessy N., Mulyadi F., Firdaus M.I., 2024. Relationship between chlorophyll-a, rainfall, and climate phenomena in tropical archipelagic estuarine waters. Heliyon, 10(4). Doi: 10.1016/j.heliyon.2024.e25812.

Taufiqurrahman E., Ismail M.F.A., 2020. Distribution of Chlorophyll-a Associated with Eddy Circulation in the Strait of Madura. OLDI, 5(2), 93–103. Doi: 10.14203/2020-v5i2-308 (in Bahasa).

Toding J.E., Widagdo S., Bintoro R.S., 2022. Variability of Sea Surface Temperature, Salinity, and Rainfall During the El Niño-Southern Oscillation (ENSO) Period in the Madura Strait Waters. Jurnal Riset Kelautan Tropis (Journal of Tropical Marine Research)(J-Tropimar), 4(1), 52–66. Doi: 10.30649/jrkt.v4i1.60 (in Bahasa).

Trinugroho T., Satriadi A., Muslim M., 2019. Distribution of Seasonal Thermal Front in Madura Strait Waters using Single Image Edge Detection. Journal of Marine Research, 8(4), 416–423. Doi: 10.14710/jmr.v8i4.24815.

Watanabe F., Alcantara E., Rodrigues T., Rotta L., Bernardo N., Imai N., 2018. Remote Sensing of the Chlorophyll-a based on OLI/Landsat-8 and MSI/Sentinel-2A (Barra Bonita reservoir, Brazil). Anais da Academia Brasileira de Ciências, 90(2), 1987–2000. Doi: 10.1590/0001-3765201720170125.

Wirasatriya A., Susanto R.D., Kunarso K., Jalil A.R., Ramdani F., Puryajati A.D., 2021. Northwest monsoon upwelling within the Indonesian seas. International Journal of Remote Sensing, 42(14), 5433–5454. Doi: 0.1080/01431161.2021.1918790.

Xiong X., et al., 2023. Aqua MODIS: 20 years of on-orbit calibration and performance. Journal of Applied Remote Sensing, 17(3), 037501–037501. Doi: 10.1117/1.JRS.17.037501.

Xu T.F., et al., 2021. Observed water exchange between the South China Sea (Easst Sea) and Java Sea through Karimata Strait. Journal of Geophysical Research: Oceans, 126, e2020JC016608. https://doi.org/10.1029/2020JC016608.

Yuliardi A.Y., Prayogo L.M., Joesidawati M.I., 2022. Dynamics of the Spatial-Vertical Distribution of Water Masses in the West and East Indonesian Throughflow Routes in the Wet Season. Jurnal Miyang: Ronggolawe Fisheries and Marine Science Journal, 2(2), 38–46. Doi: 10.55719/jmiy.v2i2.532 (in Bahasa).

Yuliardi A.Y., Rahman H.A., Sari R.J., Rahmalia D.A., Nugroho A.T., Prayogo L.M., 2024. Analysis of Seasonal Variations of Temperature, Salinity, and Surface Currents in Madura Waters. Indonesian Journal of Oceanography, 6(4), 292–305. Doi: 10.14710/ijoce.v6i4.24477 (in Bahasa).

Zainab S., Handajani N., Wibisana H., 2020. Mapping of Sea Surface Temperature and its Correlation with Salinity Concentration in The Coastal Beach of Bangkalan Madura District. In IOP Conference Series: Earth and Environmental Science. IOP Publishing, 506(1), 012050. Doi: 10.1088/1755-1315/506/1/012050.

Zhang Y., Wu Z., Liu M., He J., Shi K., Wang M., Yu Z., 2014. Thermal structure and response to long-term climatic changes in Lake Qiandaohu, a deep subtropical reservoir in China. Limnology and Oceanography, 59(4), 1193–1202. Doi: 10.4319/lo.2014.59.4.1193.